Electromagnetic Servoing—A New Tracking Paradigm

Tobias Reichl*, José Gardiazabal, and Nassir Navab

***Abstract*—Electromagnetic (EM) tracking is highly relevant for many computer assisted interventions. This is in particular due to the fact that the scientific community has not yet developed a general solution for tracking of flexible instruments within the human body. Electromagnetic tracking solutions are highly attractive for minimally invasive procedures, since they do not require line of sight. However, a major problem with EM tracking solutions is that they do not provide uniform accuracy throughout the tracking volume and the desired, highest accuracy is often only achieved close to the center of tracking volume. In this paper, we present a solution to the tracking problem, by mounting an EM field generator onto a robot arm. Proposing a new tracking paradigm, we take advantage of the electromagnetic tracking to detect the sensor within a specific sub-volume, with known and optimal accuracy. We then use the more accurate and robust robot positioning for obtaining uniform accuracy throughout the tracking volume. Such an EM servoing methodology guarantees optimal and uniform accuracy, by allowing us to always keep the tracked sensor close to the center of the tracking volume. In this paper, both dynamic accuracy and accuracy distribution within the tracking volume are evaluated using optical tracking as ground truth. In repeated evaluations, the proposed method was able to reduce the overall error from 6.64 ± 7.86 mm to a significantly improved accuracy of 3.83 ± 6.43 mm. In addition, the combined system provides a larger tracking volume, which is only limited by the reach of the robot and not the much smaller tracking volume defined by the magnetic field generator.**

***Index Terms*—Instrument and patient localization and tracking, motion modeling and compensation, planning and image guidance of interventions, robotics and human–robot interaction.**

I. Introduction

ELECTROMAGNETIC (EM) tracking is relevant for many clinical applications, including colonoscopy [1], neuroendoscopy [2], bronchoscopy [3], and catheter navigation [4], [5], and there are several clinically established and commercially available navigation solutions based on EM tracking (Biosense Webster CARTO, Medtronic StealthStation, superDimension iLogic, etc.).

Besides EM tracking, there is not yet a general solution for tracking of *flexible* instruments or endoscopes within the human body. However, in general EM tracking systems do not yet provide the same level of accuracy as optical tracking systems. The accuracy is also not uniform through the volume of interest and they are susceptible to distortions from secondary EM fields, which are caused by metallic objects in the vicinity. Consequentially, any improvement over current solutions will have an impact. Due to a missing line of sight, optical tracking is not applicable for tracking inside the human body. When flexible instruments are used, the position and orientation of parts inside the body can not be inferred from tracking of parts outside the body.

Upcoming technologies like fiber-optic tracking (Luna Technologies, Blacksburg, VA, USA) or radio-frequency identification (RFID) technology [6], [7] are promising, but their clinical tracking performance cannot be judged yet. Prototypes for time-of-flight real-time ultrasound catheter localization have been reported [8] with an internal ultrasound pulser and an external array of sensors, but their accuracy is limited to 2–3 mm due to variations of speed of sound in human tissue.

To improve EM tracking accuracy there have been numerous approaches towards the compensation of static errors [9], but these require a lengthy calibration procedure and do not hold up in a highly dynamic environment like an operating room (OR). Other approaches towards dynamic error compensation employ other sources of information like segmentation [10], image registration [11], or hybrid EM-optical tracking and models of instrument motion [12]. These approaches are highly application-specific, rely on static preoperative images, or are not yet feasible in real-time.

Here, we present a *novel* and *general* solution for improving EM tracking accuracy, which may be applicable to a sizable spectrum of interventions, including colonoscopy, neuroendoscopy, bronchoscopy, and catheter navigation. Rogers *et al.* [13] presented an ultrasound-holding needle biopsy robot, with movement commands determined from segmentation results. However, in their set-up, the tracked object's position was only determined at a single point in time, and tracking was neither the focus nor the objective of their valuable work.

We use electromagnetic tracking to detect a sensor within a small, specific sub-volume, with known and optimal accuracy, where no line of sight is available. Then we use a robotic arm to reposition the field generator, in order to maximize the accuracy of the electromagnetic tracking. This combines the best

Manuscript received February 20, 2013; revised April 19, 2013; accepted April 19, 2013. Date of publication April 24, 2013; date of current version July 27, 2013. This work was supported in part by the European Union FP7 under Grant 256984, in part by Deutsche Forschungsgemeinschaft SFB 824, and in part by the TUM Graduate School of Information Science in Health (GSISH). *Asterisk indicates corresponding author.*

*T. Reichl is with Computer Aided Medical Procedures (CAMP), Technische Universität München, 85748 Munich, Germany (e-mail: reichl@tum.de).

J. Gardiazabal is with Computer Aided Medical Procedures (CAMP), Technische Universität München, 85748 Munich, Germany, and also with the Department of Nuclear Medicine, Klinikum rechts der Isar, Technische Universität München, 85748 Munich, Germany (e-mail: gardiaza@in.tum.de).

N. Navab is with Computer Aided Medical Procedures (CAMP), Technische Universität München, 85748 Munich, Germany (e-mail: navab@cs.tum.edu).

Color versions of one or more of the figures in this paper are available online at http://ieeexplore.ieee.org.

Digital Object Identifier 10.1109/TMI.2013.2259636

0278-0062/$31.00 © 2013 IEEE

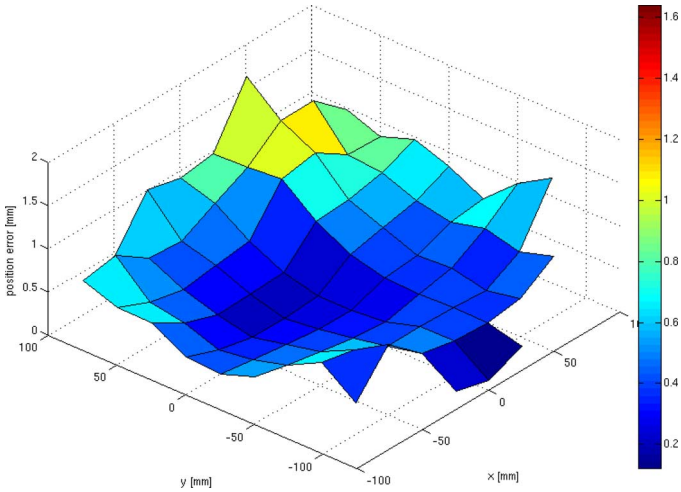

Fig. 1. Typically bowl-shaped plot of absolute three-dimensional tracking position accuracy (right), as distributed in x and y direction.

of both methods, namely tracking without a line of sight with electromagnetic tracking, and uniform and higher tracking accuracy with robot positioning. This approach is superior to hybrid optical and electromagnetic tracking [12], [14], since with such hybrid tracking there will still be suboptimal positions of the EM sensor relative to the field generator.

Our method does not rely on the assumption of static error, but it can still be freely combined with and take advantage of existing methods for static error correction.

We do introduce additional complexity into the OR, but we do so in order to gain accuracy. The robot does not need to touch the patient, and during endoscopic or catheter navigation—exactly, where EM tracking is needed, in contrast to open surgery—the space directly above the patient is free, and the robot could be attached to the OR bed, a movable small and lightweight cart, or the ceiling. Depending on the application, the robot could even be placed under the OR bed.

During bronchoscopic examinations or cardiac catheterization, the robot can keep the EM field generator close to the chest of the patient, without actually touching it. During gastroscopy or colonoscopy, the robot can keep the EM field generator close to the abdominal surface. The robot could be used not only for tracking, but also for carrying imaging devices like ultrasound transducers [15] or oxygen sensing probes [16], which could then be co-registered through our method with tracked tools. However, in such cases further research is necessary for adoption of technology taking interferences between the systems into account.

Ideally, optical tracking would be used, when a line of sight is available, and electromagnetic servoing, when no line of sight is available.

Tracking accuracy delivered by current EM tracking solutions is not uniform throughout the tracking volume, as shown in Fig. 1. The highest accuracy is commonly found close to the center of the tracking volume. Thus, our approach aims at always maintaining this ideal relative positioning of EM field generator and sensor. Since such a feedback loop could hardly be realized with a human operator in this loop, the field generator is moved in an automated manner by a robotic arm. Such *EM-servoed tracking* results in uniform and optimal EM tracking accuracy, only diminished by robotic relative accuracy, which is usually negligible in comparison to EM tracking accuracy. As an additional benefit, the effective tracking volume is increased, and is no longer limited by the EM field, but by the reach of the robot.

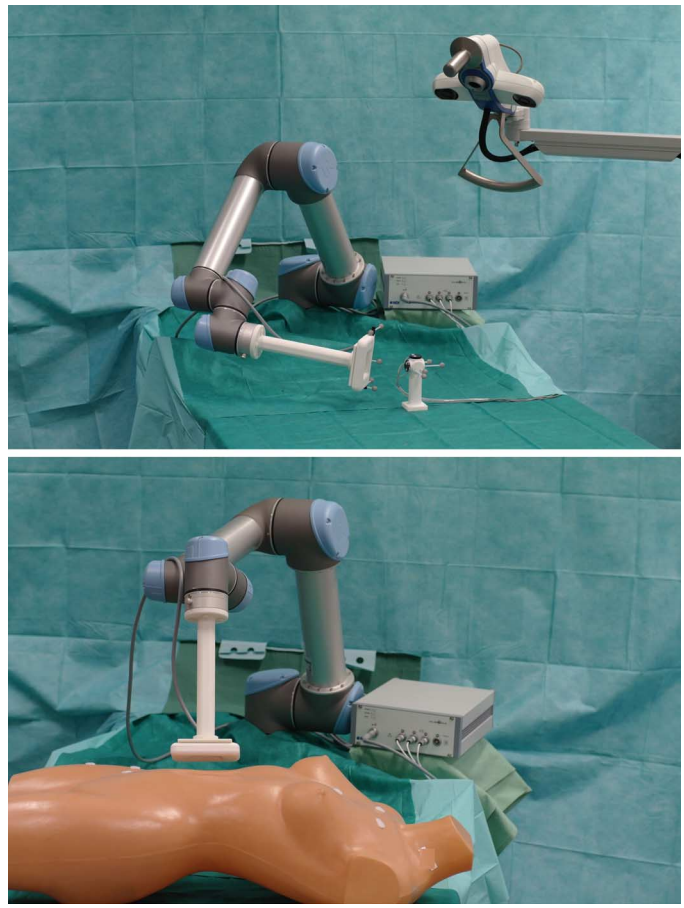

Fig. 2. Evaluation setup (top), arranged for display purposes, and mock-up setup (bottom) for tracking during abdominal intervention.

II. Methods

Our setup, as shown in Fig. 2, consists of a six-axis robotic arm (UR-6-85-5-A, Universal Robots, Odense, Denmark, stated accuracy 0.1 mm) and an EM tracking system (Aurora, Northern Digital, Waterloo, ON, Canada) with a compact field generator (stated accuracy 0.6 mm). For evaluation purposes we also use an optical tracking system (Polaris Vicra, Northern Digital, Waterloo, ON, Canada, stated accuracy 0.25 mm) and the tracking targets were kept near the optical tracking volume center to minimize the error. The range of motion in our experiments was similar to the tracking volume of the EM field generator (diameter 220 mm, height 185 mm, see Fig. 4), and thus the tracking volume of the Polaris Vicra[1] (width 491–938 mm, depth 779 mm) was sufficient.

The EM field generator was rigidly fixed to the robot hand using a custom-designed spacer made of bio-compatible DuraForm PA plastic, which is shown in Fig. 3. For evaluation

[1]http://www.ndigital.com/medical/polarisfamily-volumes-vicra.php

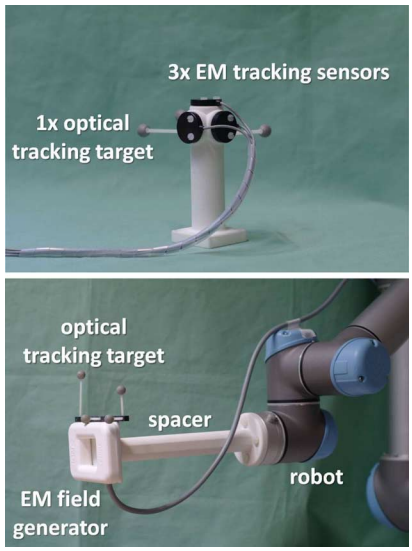

Fig. 3. EM sensors mounted in orthogonal orientations (top), and EM field generator attached to robot (bottom), both equipped with optical tracking targets for evaluation.

three EM sensors were fixed in orthogonal orientations to a holder made of the same material. Two nonmetallic optical tracking targets were attached to both the EM field generator and to the EM sensors.

It can be derived from theoretical considerations that secondary EM fields from any metallic object, whose distance from the EM field generator is at least twice the distance between EM field generator and sensor, contributes less than 1% to the measured field strength [17]. Since our goal is to track an object at the center of the tracking volume, the distance between EM field generator and sensor is kept at approximately 95–100 mm. Thus, a spacer of 220 mm length between robot and EM field generator is sufficient to avoid EM distortions from the robot.

Polyamide screws were used in the vicinity of the EM field generator and EM sensors. Evaluations were performed over a metal-free table, with as much distance from other electrical equipment (computers, power supplies, lamps, etc.) as possible.

A. Hand–Eye Calibration

We perform hand–eye calibration as proposed by Tsai and Lenz [18]. Measurements during a sequence of robot hand motions can be rewritten as $A \cdot X = X \cdot B$ or

$$ {}^{\acute{H}}\mathbf{M}_H \cdot {}^{H}\mathbf{T}_F = {}^{H}\mathbf{T}_F \cdot {}^{\acute{F}}\mathbf{M}_F \tag{1} $$

where $A = {}^{\acute{H}}\mathbf{M}_H$ is a motion of the robot hand relative to the robot base, $B = {}^{\acute{F}}\mathbf{M}_F$ is the corresponding, measured motion of the EM field generator relative to a fixed sensor, and $X = {}^{H}\mathbf{T}_F$ is the transformation from the EM field generator to the robot hand.

Using input motions from robot positioning, EM tracking, and optical tracking for the hand–eye calibration algorithm, it is possible to compute the fixed transformations in our setup. We are particularly interested in the transformation matrix ${}^{H}\mathbf{T}_F$ from the EM field generator to the robot hand, and in the transformation ${}^{T}\mathbf{T}_S$ from the EM sensors to the optical tracking target next to the sensors. The latter ${}^{T}\mathbf{T}_S$ is computed from motions $A = {}^{\acute{T}}\mathbf{T}_T$ of the optical tracking target relative to the optical tracking system and from motions $B = {}^{\acute{S}}\mathbf{T}_S$ of the EM sensor relative to the field generator. These relative motions can be computed, even though the EM sensor and the optical tracking target are stationary during hand–eye calibration. It is important to note that the transformation ${}^{T}\mathbf{T}_S$ is only relevant for comparing ground truth for evaluation, and our setup does not depend on optical tracking.

The robot hand serves as a dynamic reference frame for EM tracking, after the pose of the EM field generator ${}^{H}\mathbf{T}_F$ relative to the robot hand has been calibrated. The additional optical tracking target is only included for evaluation purposes.

Hand–eye calibration is fully automated and takes only seconds to perform.

B. Feedback Loop and EM Servoing

In order to keep the EM sensor at the center of the tracking volume, its position is constantly monitored. During tracking arbitrarily many position changes may be expected, so manual motion is not applicable. For example, we observed during bronchoscopy procedures on patients that motion is usually confined to a volume of 200 × 200 × 100 mm. However, there is a lot of movement of the bronchoscope due to steering and breathing motion, and thus the overall distance traveled during an inspection of the central airways can be one meter and more. Whenever the distance from a preselected position is larger than a specified threshold, the required translation vector ${}^{\acute{F}}\mathbf{t}_F$ of the field generator is computed and the robot hand pose ${}^{B}\mathbf{T}_H$ is updated as

$$ {}^{B}\acute{\mathbf{T}}_H = {}^{B}\mathbf{T}_H \cdot {}^{H}\mathbf{T}_F \cdot \begin{bmatrix} I & {}^{\acute{F}}\mathbf{t}_F \\ \vec{0} & 1 \end{bmatrix} \cdot \left({}^{H}\mathbf{T}_F\right)^{-1} \tag{2} $$

where ${}^{B}\mathbf{T}_H$ is the transformation from robot hand to base and ${}^{H}\mathbf{T}_F$ is the transformation from the field generator to the robot hand. The new hand pose ${}^{B}\acute{\mathbf{T}}_H$ is then sent to the robot and executed. Ultimately, the field generator would move continuously.

This method can be implemented with any particular preselected position within the tracking volume, and any specified threshold. The volume center was chosen as the point of highest static accuracy, and we will demonstrate below, how to define the threshold based on static tracking accuracy measurements.

This method can be freely combined with existing methods for static error correction [9], but our method does not depend on a calibration of static errors, but on the motion through the robot, and thus it is different from previous methods. If such an error correction method is available, it can be used to look up the previously determined, corrected values for EM tracking, before computing the required translation vector ${}^{\acute{F}}\mathbf{t}_F$.

III. Experiments and Results

Hand–Eye calibration: In 54 repetitions of the hand–eye calibration procedure, the results for the transformation ${}^{H}\mathbf{T}_F$ from field generator to robot hand had a mean deviation from their mean of 1.91 mm and 2.55°, i.e., less than one percent of the true distance of 243 mm.

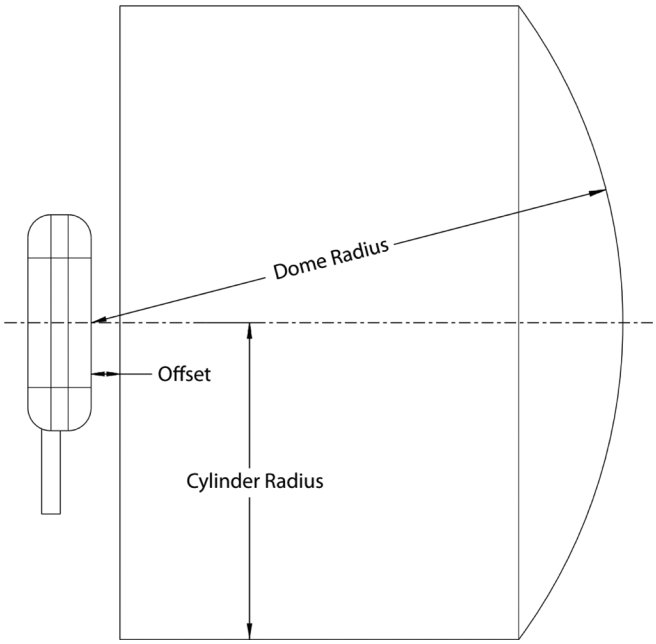

Fig. 4. Tracking volume of compact field generator, where volume offset is 10 mm, cylinder radius is 110 mm, and dome radius is 185 mm. Image courtesy of Northern Digital [24].

A. Static Data Acquisition

In order to verify that our setup does not introduce additional errors, we determine static EM tracking accuracy first. There have been numerous works benchmarking EM tracking systems and assessing EM field inhomogeneities, e.g., [19]–[23]. We employ a standard methodology for evaluation of the setup, which is analogous to these previous works, and involves registration to ground truth data from optical tracking.

The scanning volume was defined according to the field generator specifications [24] with a cylinder radius of 110 mm and a dome radius of 185 mm (cf. Fig. 4) and transformed into robot coordinates using hand–eye calibration results (cf. Section II-A). The sensors remained static, while the field generator was moved through the tracking volume without changing its orientation. The volume was sampled on a regular 3-D grid with a spacing of 25 mm, and 10 samples were recorded at each position. In order to avoid bias due to sensor orientation, we used three sensors at the same time, which were mounted in orthogonal orientations, cf. Fig. 3.

For all $i \in 1 \cdots n$ stations, the EM tracking measurements ${}^{F}\mathbf{T}_{S,i}$ were transformed into the robot base coordinate system $\mathbf{B}$ as

$$ {}^{B}\mathbf{T}_{S,i} = {}^{B}\mathbf{T}_{H} \cdot {}^{H}\mathbf{T}_{F} \cdot {}^{F}\mathbf{T}_{S,i} \tag{3} $$

where ${}^{B}\mathbf{T}_{H}$ is the current robot hand pose, and ${}^{H}\mathbf{T}_{F}$ is the calibrated transformation from EM field generator to robot hand. Optical tracking was used as ground truth, and since the spatial relation ${}^{T}\mathbf{T}_{S}$ between the EM sensors and the optical tracking target is known, a reference value ${}^{O}\mathbf{T}_{S,i}$ for the EM sensor's pose relative to the optical tracking system can be determined as

$$ {}^{O}\mathbf{T}_{S,i} = {}^{O}\mathbf{T}_{T,i} \cdot {}^{T}\mathbf{T}_{S} \tag{4} $$

where ${}^{O}\mathbf{T}_{T,i}$ is the current optical tracking measurement for the tracking target.

The spatial relation ${}^{B}\mathbf{T}_{O}$ between optical tracking system and robot base is available as a by-product of hand–eye calibration. However, we optimized the hand poses used for hand–eye calibration for an accurate determination of ${}^{H}\mathbf{T}_{F}$, and due to the large distance of approximately 1.3 m between optical tracking system and robot base, position uncertainty for ${}^{B}\mathbf{T}_{O}$ is higher (up to several centimeters) than for ${}^{H}\mathbf{T}_{F}$. Thus, we do not use the original measurement of ${}^{B}\mathbf{T}_{O}$ for evaluation of position errors.

Instead, as proposed by earlier works on tracking system benchmarking ([19], [23]), the transformation ${}^{B}\mathbf{T}_{O}^{*}$ between reference positions ${}^{O}\mathbf{p}_{S}$ relative to optical tracking, and positions ${}^{B}\mathbf{p}_{S}$ relative to the robot base was computed by point-based registration as

$$ {}^{B}\mathbf{p}_{S} = {}^{B}\mathbf{T}_{O}^{*} \cdot {}^{O}\mathbf{p}_{S}. \tag{5} $$

Position errors can then be computed as Euclidean distances between measured positions ${}^{B}\mathbf{p}_{S,i}$ and transformed positions ${}^{O}\mathbf{p}_{S,i}$.

For optimal registration, we picked the 10% of measurement points with best signal quality (quality as reported by the tracking system), since this ratio seems to avoid both over- and underestimation. If too few points are used for point-based registration (or if these points' accuracy is worse than average), measurement errors in these points may lead to an overestimation of errors for the remaining points. However, if too many points are used, this may lead to an underestimation, since the errors are minimized during registration. We verified that any other percentage between 1% and 99% did not change the final result by more than 0.06 mm.

For evaluation of orientation errors, it is possible to use the original measurement of ${}^{B}\mathbf{T}_{O}$ from hand–eye calibration, since orientation errors do not scale with distance. Thus, we compute a reference pose ${}^{B}\acute{\mathbf{T}}_{S,i}$ of the EM sensor relative to the robot base as

$$ {}^{B}\acute{\mathbf{T}}_{S,i} = {}^{B}\mathbf{T}_{O} \cdot {}^{O}\mathbf{T}_{T,i} \cdot {}^{T}\mathbf{T}_{S}. \tag{6} $$

Orientation difference was then determined as the angle between orientation of measured pose ${}^{B}\mathbf{T}_{S,i}$ [cf. Equation (3)] and orientation of reference pose ${}^{B}\acute{\mathbf{T}}_{S,i}$.

The static accuracy of our tracking setup, including co-calibration of EM tracking and optical tracking for evaluation, was 1.55 ± 0.62 mm and $1.46 \pm 1.07°$ over the whole tracking volume, which is shown in Fig. 4.

The field generator was moved in three dimensions across the whole tracking volume. For each measurement, the absolute 3-D position error was determined as Euclidean distance from ground truth data.

In order to show the distribution of errors across the tracking volume, errors were then collected by measurement location into bins of 25×25 mm in two direction and averaged along the third direction. In particular, there was a single bin along the third direction, in order to reduce dimensionality for visualization. The distribution of static position accuracy in our set-up is shown in Fig. 5.

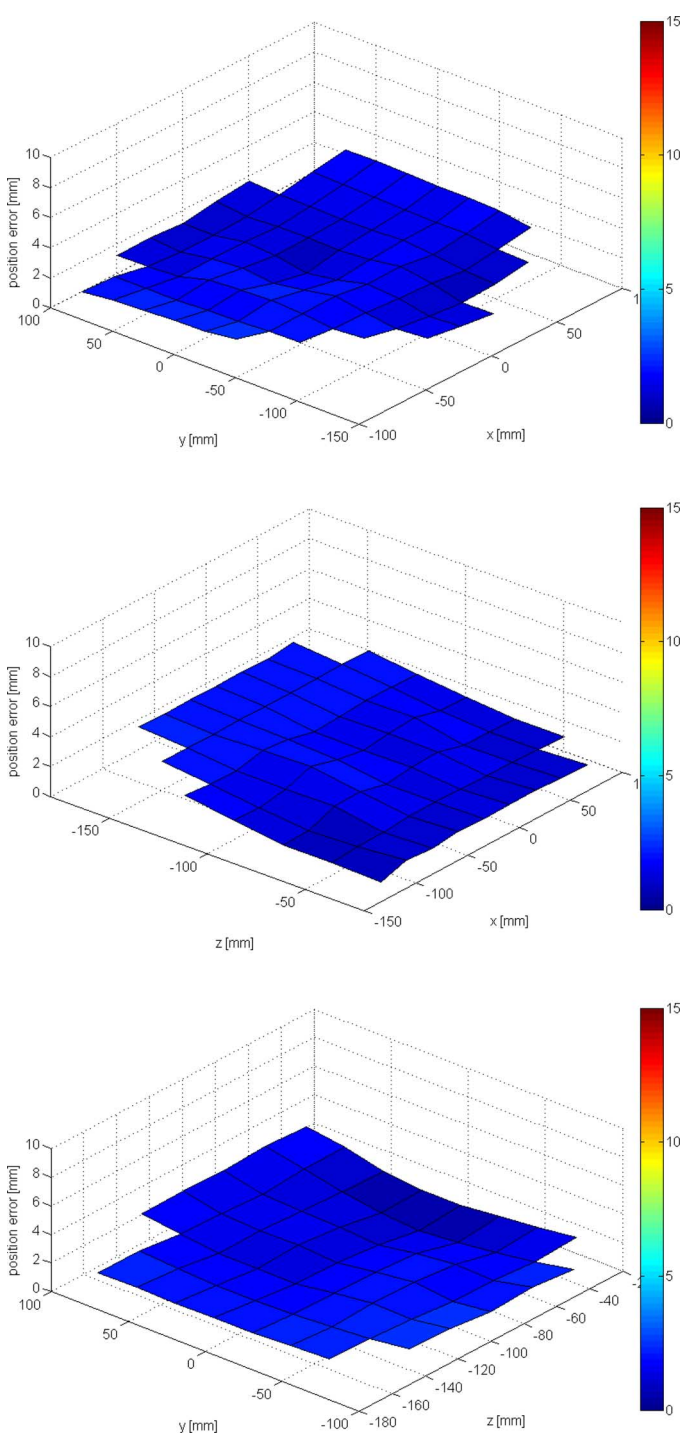

Fig. 5. Absolute static 3-D tracking position accuracy in our setup, as distributed in x and y direction (top), x and z direction (middle), or y and z direction (bottom).

The relationship between distance of the EM tracking sensor from the tracking volume center and the position error is shown in Fig. 6. We fitted a quadratic function to the measured performance within a distance of up to 50 mm. From this we can derive that, in order to achieve sub-millimeter accuracy, the distance from the tracking volume center needs to be kept below 20.35 mm. Beyond this distance a steep increase in error can be seen, and thus in our evaluation 20 mm was chosen as motion

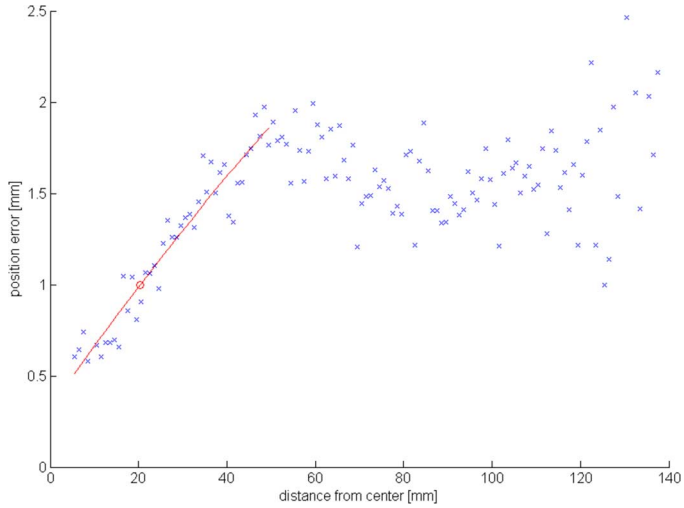

Fig. 6. Static position error versus distance of EM sensor from the tracking volume center. We fitted a quadratic function to the measured performance within a distance of up to 50 mm (red line). Distance of up to 20.35 mm corresponds to sub-millimeter accuracy (red circle), and with greater distances the error steeply increases.

threshold. The threshold could also be set to zero, i.e., having the robot continuously moving, but since the dynamic tracking accuracy of EM tracking is limited to one millimeter in the best case (cf. Fig. 12), there is no need for a lower threshold. The threshold could be set higher, though, in order to come to a compromise achieving the desired accuracy, while reducing the motion of the robot.

B. *"Pure" Tracking Accuracy*

For an assessment of "pure" static tracking error (as given by tracking system manufacturers) without calibration error, it is also possible to perform a point-based registration of positions measured by EM and optical tracking, without inclusion of ${}^{T}\mathbf{T}_{S}$, as proposed by e.g., [19], [22], [23]. This transformation does not have a physical meaning, since the assumption is that EM and optical measurements describe the same point in space, which they do not. However, position error can then be determined as Euclidean error between originally measured positions and transformed reference positions. The orientation error can be determined as the mean deviation from the average measured orientation, since the true orientation of both the sensors and the field generator remained constant. In five separate experiments on three different days we measured a mean static position error between 0.54 and 0.68 mm, and a mean static orientation error between 0.49° and 0.67°, which agrees with the specified accuracy for the EM tracking system (0.6 mm and 0.8°), cf. Fig. 7. This confirms that the robot does not adversely influence tracking accuracy.

The same assessment can also be performed using the more accurate robot positioning data instead of optical tracking, yielding a mean static position error between 0.51 and 0.74 mm, and again a mean static orientation error between 0.49° and 0.67°. This agrees with the result using optical tracking and confirms that optical tracking can be used for evaluation of our method.

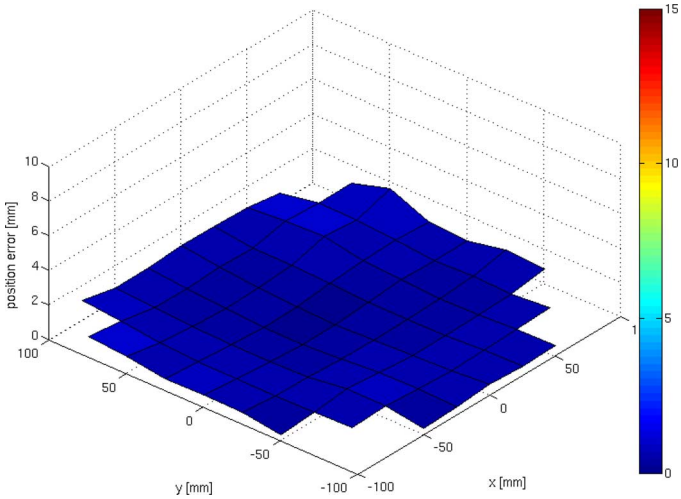

Fig. 7. Pure absolute 3-D tracking position accuracy in our setup, as distributed in x and y direction.

TABLE I
DYNAMIC TRACKING ACCURACY DURING FOUR EXPERIMENTS EACH WITH STATIONARY FIELD GENERATOR (FG, TRADITIONAL SETUP) AND MOVING FIELD GENERATOR (ELECTROMAGNETIC SERVOING). ELECTROMAGNETIC SERVOING SIGNIFICANTLY IMPROVES TRACKING ACCURACY. STATIC TRACKING ACCURACY IS SHOWN FOR COMPARISON

	Position accuracy	Orientation accuracy
Dynamic, stationary FG	$6.64 \pm 7.86\,mm$	$2.70 \pm 1.56°$
Dynamic, moving FG	$3.83 \pm 6.43\,mm$	$1.34 \pm 0.52°$
Static acquisition	$1.55 \pm 0.62\,mm$	$1.46 \pm 1.07°$

C. Dynamic Data Acquisition

In order to evaluate the accuracy of EM-servoing, we moved the EM sensors by hand, while the robot was following one of the sensors. We were covering the full tracking volume and a range of speeds between 0 and 100 mm/s, which for example covers clinically relevant speeds of flexible endoscopes. As described in Section II-B, whenever the sensor was detected more than 20 mm away from the center of the tracking system, the robot would move accordingly and refocus on the sensor. In particular, the robot would move in three dimensions, depending on sensor movement.

For comparison with the traditional setup with a fixed field generator, in another type of experiment the robot remained *static*, while measurements were recorded. Both cases were evaluated against optical tracking as ground truth data.

Measurements were performed with either a moving field generator or with a static field generator. More than 136 000 samples were collected for each case, where each sample consisted of corresponding measurements for all EM sensors and optical targets as well as the robot.

The position and orientation accuracy determined for both cases are compared in Table I, together with the static acquisition. In total, the proposed method was able to reduce the mean error from 6.64 mm and 2.70° to 3.83 mm and 1.34°. Assuming that the three components of position error vectors are normally distributed, the overall Euclidean position error follows a χ_3 distribution, also known as Maxwell–Boltzmann distribution. Approximating this by a normal distribution, we may use Welch's t-test, which yields $p \ll 0.001$, i.e., due to the large number of measurements, the difference is statistically highly significant. The accuracy distribution over the tracking volume is shown in Fig. 8.

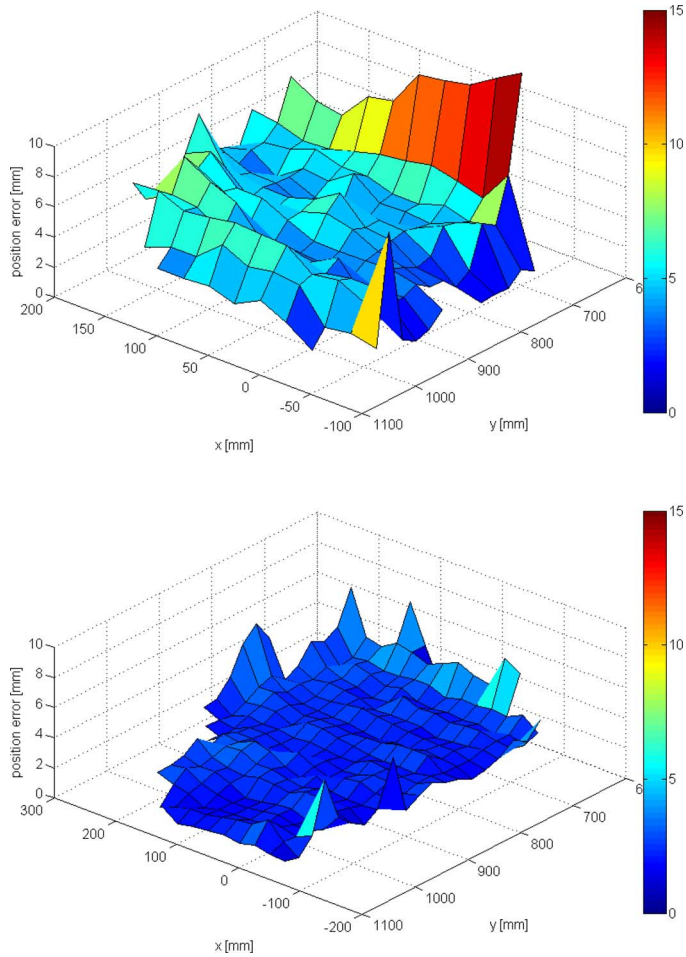

Fig. 8. Dynamic absolute 3-D position errors of traditional setup with static field generator (top) and proposed method with moving field generator (bottom), as distributed in x and y direction. Please note that the proposed method provides mostly uniform errors across the tracking volume, as well as a larger tracking volume. For visualization, 10% outliers have been removed in both plots.

D. Outlook: Medical Application

In order to demonstrate the potential application of our method, we performed EM servoing and tracked a flexible catheter within a realistic bronchoscopy phantom. EM tracking has already been clinically established for navigated bronchoscopy [3] and approved devices like iLogic (superDimension, Minneapolis, MN, USA) are commercially available. Our set-up for the navigated bronchoscopy application is depicted in Fig. 9. We used a bronchoscopy training phantom with realistic shape and appearance (Koken, Tokyo, Japan), which is usually used for the training of bronchoscopists. Similar to the workflow proposed by Maurer *et al.* [25] registration of the phantom to tracking data was performed via optical tracking markers, which were also well visible in the computed tomography (CT) image. After point-based registration of marker positions in image space and tracking space [25], the position and orientation of a tracked 6-D catheter (Aurora, Northern Digital, Waterloo, ON, Canada) can be visualized directly in

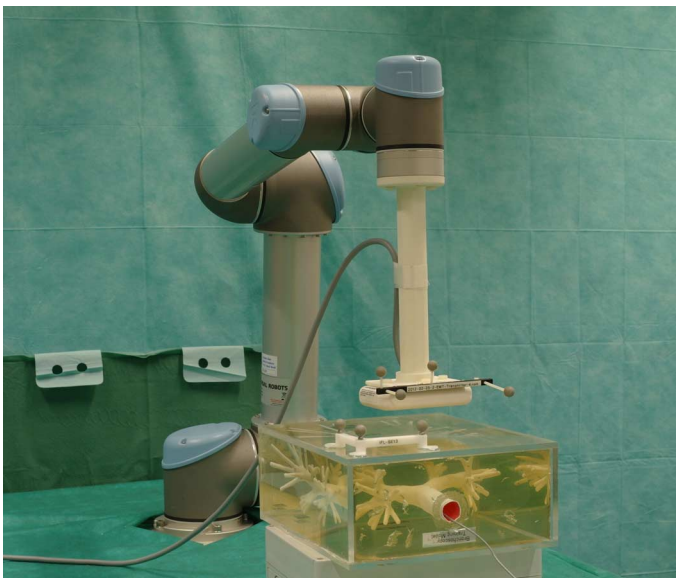

Fig. 9. Setup for medical application demonstration. A flexible catheter was inserted into a realistic bronchoscopy training phantom and tracked using EM servoing. As with a real intervention, a registration between the phantom CT image and tracking coordinates is required, for which we used optical tracking markers, which were also well visible in the CT image.

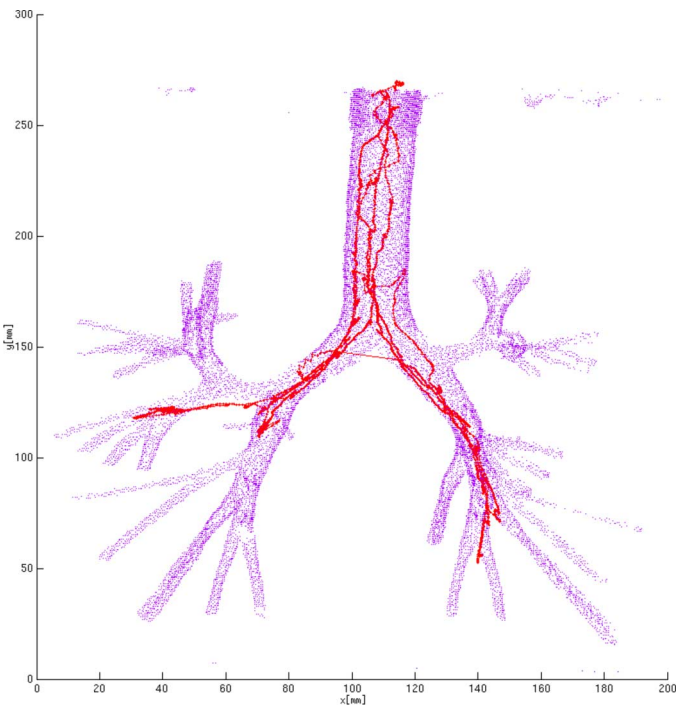

Fig. 10. Trajectory of an EM tracked catheter (red line) is visualized with respect to the airway shape as extracted from CT data (blue). It can be seen qualitatively that the trajectory is almost completely within the airway lumen.

relation to CT data. In Figs. 10 and 11 we show the catheter's recorded trajectory in relation to a segmentation of the airway shape—for segmentation, a gradient threshold was used. Inside the airways no ground truth for the tracking of the flexible catheter is available. However, it can be seen qualitatively that the trajectory is almost completely within the airway lumen.

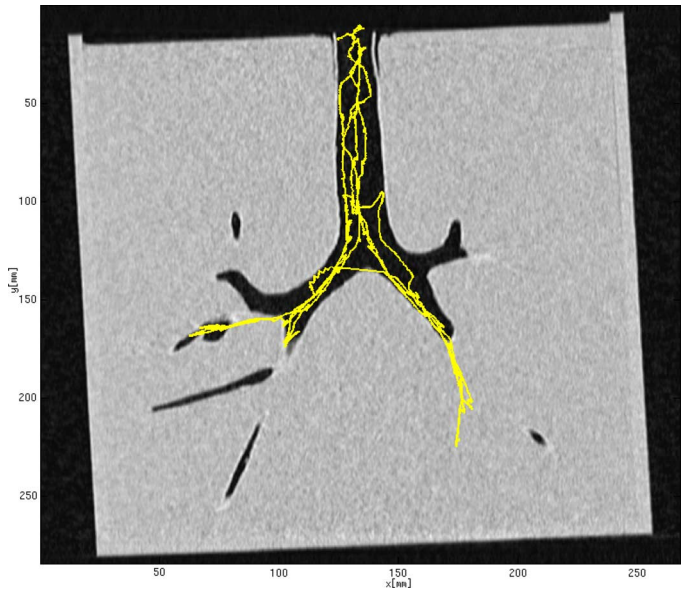

Fig. 11. Trajectory of an EM tracked catheter (yellow line) can be overlaid over slices from the CT image itself—please note that here the full trajectory is visualized, even where actually in front of or behind the chosen CT slice.

IV. Discussion

Multiple EM sensors can be tracked at the same time, i.e., all sensors within the EM tracking volume. However, a meaningful EM servoing objective needs to be chosen. Either a single sensor can be kept close to the tracking center, or several sensors, if they are close together.

Interpretation of EM tracking error components: The difference between the dynamic acquisition with static (6.64 mm) and moving field generator (3.83 mm) indicates the error due to increased distance from the center of the tracking volume (diminished by additional error due to robot movement, which we assume to be negligible). This component amounts to 2.81 mm on average. The correlation between distance from the center of the tracking volume and position error is demonstrated in Fig. 12 for a continuous acquisition of more than 34 000 samples with stationary field generator, where this correlation was clearly visible. There, measurements were binned by distance from the center of the tracking volume, and average position error was computed. A similar correlation was observed in the quasi-static acquisition, but the effect is significantly stronger for dynamic measurements, leading to higher error. Over the whole dynamic acquisition data set with stationary field generator, the correlation coefficient between distance from the center of the tracking volume and the position error was 0.87.

Further error is due to the motion of the EM sensor during measurement. This can be explained if the transmit coils of the EM field generator are sequentially excited, i.e., for each tracking update, multiple readings of electromagnetic fields are taken in sequence and combined into position and orientation estimates. However, this needs to be further evaluated with different magnetic tracking systems. In this case there is one measurement for all sensor coils, while each field generator coil is active. Motion of a sensor during such a measurement cycle results in inconsistent measurements and leads to tracking errors.

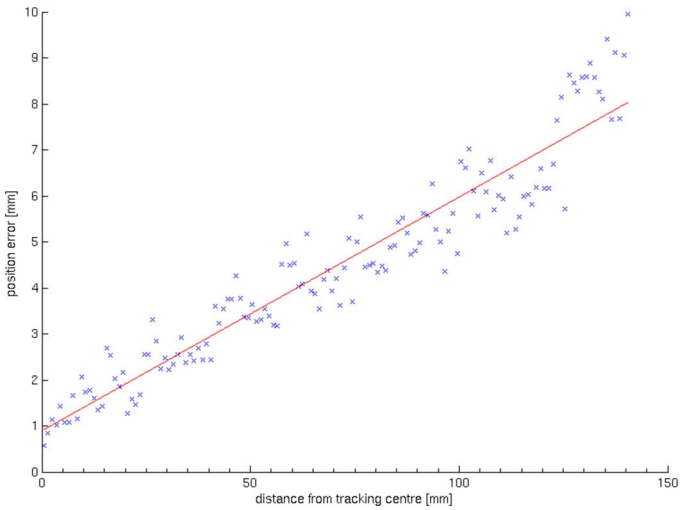

Fig. 12. Dynamic position error is correlated with Euclidean distance from the center of the tracking volume. Keeping the EM tracking sensor close to the center, as with EM servoing, significantly improves accuracy.

A relationship between motion speed and tracking accuracy has already been reported by Nafis *et al.* [21], albeit to a lesser extent for the NDI Aurora system than for other systems.

The motion-related error component can be estimated as the difference of 5.09 mm between the dynamic acquisition with static field generator (6.64 mm) and the quasi-static acquisition (1.55 mm). This difference is reduced to 2.28 mm in the dynamic acquisition with moving field generator (3.83 mm). The correlation between the sensor's positional velocity and position error is demonstrated in Fig. 13 for continuous sequences of more than 36 000 samples with both stationary and moving field generator, where this correlation was clearly visible. Measurements were binned by sensor's positional velocity, and average position error was computed. Over the whole data sets, the correlation coefficient between sensor's positional velocity and position error was 0.77 (traditional setup) and 0.71 (proposed method), but keeping the sensor close to the center of the tracking volume decreases the amount of error significantly.

While previous works [19] did already use a robotically moved EM tracking sensor, a robotically moved field generator may be used to estimate EM field inhomogeneity.[2] Even when moving an EM sensor, use of a robot promises exploration of dynamic effects, since predefined speed profiles can be used.

Hummel *et al.* [26] found dynamic position errors of 3.24 mm with a pendulum setup. However, in contrast to their setup we used three sensors mounted in orthogonal orientations, in order not to favor specific sensor orientations, and we covered the full depth of the tracking volume. Thus, we believe that the dynamic position errors observed in our experiments agree with previous results. Dynamic EM tracking errors have received little attention so far, and, besides the improvement due to the proposed method, their study is beyond the scope of our work. In the future, a fast-moving robot could be able to reduce the relative motion of EM field generator and sensor, and thus could be able to reduce motion artifacts.

[2]We would like to thank the anonymous reviewer for this suggestion.

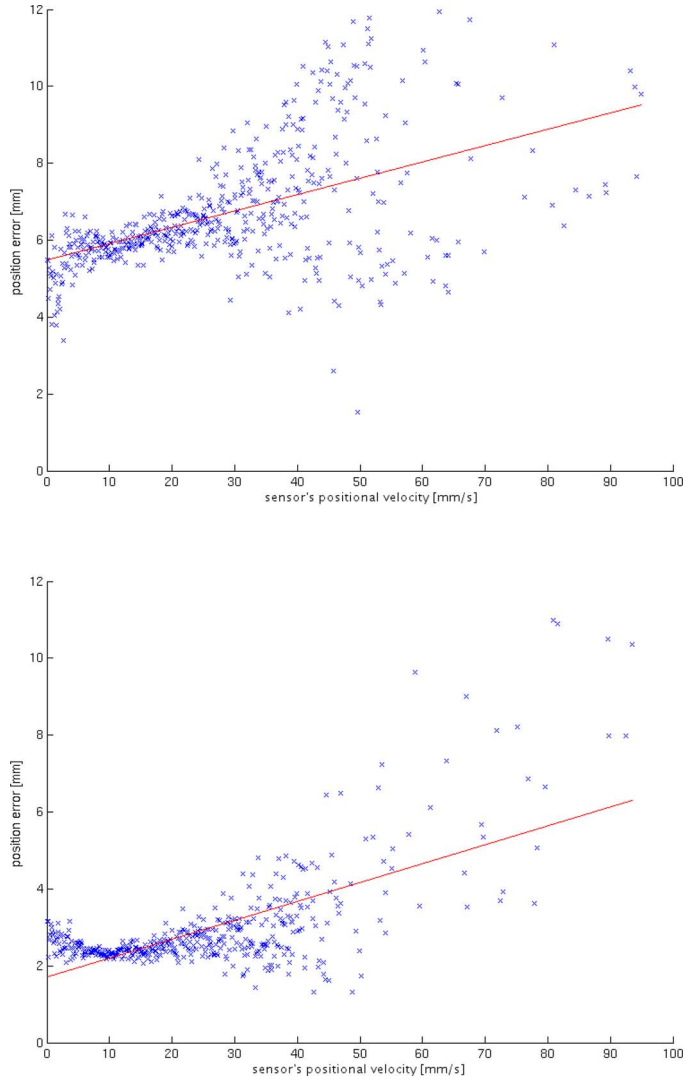

Fig. 13. Position error versus sensor velocity for measurements with stationary field generator in the traditional setup (top) or with moving field generator for EM servoing (bottom). By keeping the EM tracking sensor close to the center, the proposed method significantly improves accuracy.

NDI recently released the Aurora table-top field generator. Both the compact field generator and the table-top field generator were found to provide better accuracy than the Aurora planar field generator, within their different tracking volumes [27]. However, the resulting tracking volume of our method is only limited by the reach of the robot, and thus is possibly bigger than the tracking volume of the table-top field generator. Of course, if the tracking volume of the table-top field generator is sufficient for certain applications, then the additional complexity of introducing a robot can be saved. However, experiments have shown that the compact field generator is considerably more robust to metallic components in the environment [27]. A detailed study of the performance of EM tracking system in clinical environments has been presented by Yaniv *et al.* [22], while the influence of metals on EM tracking in general has been evaluated by Hummel *et al.* [28] and theoretically explained by Nixon *et al.* [29].

Following the considerations of distance from metals, a setup like the proposed is potentially more robust against influences

from OR tables and other items, since the distance between the field generator and sensor is small, compared to the distance between field generator and OR table. Note that metal-free OR tables with carbon fiber tops are already being used for intra-operative C-arm imaging.

The robot used in our set-up has redundant safety features generating a protective stop if the force exceeds 150 Newtons. While this is sufficient for research and development and no additional safety guards are needed between robot and operator, for use on patients further safety measures will need to be introduced [30]. Since in our application we do not need to touch the patient, contact sensors or an additional distance measurement sensor could be mounted at the EM field generator, ensuring a safe distance from the patient even in the case of errors in tracking or registration.

Even our rather low-cost robotic arm has a stated accuracy of 0.1 mm (Universal Robots), and similar specifications are given by other manufacturers (KUKA, Barrett). The particular robot in our setup was only used as proof of concept, and with a more advanced robot, several issues could be avoided. For instance, there was no suitable real-time interface available, and there was considerable temporal lag before commands were executed (up to 600 ms). Thus, the robot was only able to follow the tracked object at slow speeds, which could easily be remedied with a real-time interface. Also, the robot currently used is rather heavy (18 kg weight, 5 kg payload), and for better integration into clinical environment and workflow it could easily be replaced with a more lightweight robot, since the EM field generator weighs only 120 g. In the current implementation, electromagnetic servoing does not require more than three degrees of freedom. Thus, even simpler kinematics like selective compliant assembly robot arm (SCARA) robots could be used.

In contrast to previous works concerning hybrid EM-optical tracking [31], [32], we do not only provide a larger effective tracking volume and relocation ability of the EM field generator, but we are also able to maintain the optimal level of accuracy throughout the tracking volume, otherwise only obtained close to the tracking volume center.

V. Conclusion

We presented a novel and general solution for improving EM tracking accuracy, namely *electromagnetic servoing*.

There is a clear correlation between an EM sensor's distance from the center of the tracking volume and its position error. By keeping the sensor close to the center of the volume at all times, tracking error is significantly reduced.

We use electromagnetic tracking to detect and localize a sensor within a specific sub-volume, with known and optimal accuracy. We introduce a new tacking paradigm, which takes advantage of more accurate and robust robot positioning for obtaining uniform tracking accuracy. This leverages tracking without a line of sight by electromagnetic tracking, and uniform and higher accuracy of robot positioning.

We have shown the feasibility of the setup, and in a thorough accuracy evaluation we have shown that the mean accuracy can be significantly improved from 6.64 mm and 2.70° to 3.83 mm and 1.34°. Our method may be applicable to a sizable spectrum of interventions, including colonoscopy, neuroendoscopy, bronchoscopy, and catheter navigation.

References

[1] L. Y. Ching, K. Moller, and J. Suthakorn, "Non-radiological colonoscope tracking image guided colonoscopy using commercially available electromagnetic tracking system," in *Proc. IEEE Conf. Robot. Automat. Mechatron.*, 2010, pp. 62–67.

[2] C. Hayhurst, P. Byrne, P. R. Eldridge, and C. L. Mallucci, "Application of electromagnetic technology to neuronavigation: A revolution in image-guided neurosurgery," *J. Neurosurg.*, vol. 111, no. 6, pp. 1179–1184, 2009.

[3] R. Abdallah, T. R. Gildea, M. K. Ghanem, M. M. Metwally, M. Machuzac, P. J. Mazzone, A. H. Osman, and A. C. Mehta, "The evolution of electromagnetic navigation bronchoscopy," *Chest*, vol. 136, no. 4, pp. 85S-c–86S-c, 2009.

[4] M.-O. Eriksson, A. Wanhainen, and R. Nyman, "Intravascular ultrasound with a vector phased-array probe (acunav) is feasible in endovascular abdominal aortic aneurysm repair," *Acta Radiologica*, vol. 50, no. 8, pp. 870–875, 2009.

[5] Y. Khaykin *et al.*, "CARTO-guided vs. NavX-guided pulmonary vein antrum isolation and pulmonary vein antrum isolation performed without 3-D mapping," *J. Intervent. Cardiac Electrophysiol.*, vol. 30, pp. 233–240, 2011.

[6] C. Hekimian-Williams, B. Grant, X. Liu, Z. Zhang, and P. Kumar, "Accurate localization of RFID tags using phase difference," in *Proc. IEEE Int. Conf. RFID*, Apr. 2010, pp. 89–96.

[7] A. Wille, M. Broll, and S. Winter, "Phase difference based RFID navigation for medical applications," in *Proc. IEEE Int. Conf. RFID*, Apr. 2011, pp. 98–105.

[8] J. Mung, S. Han, and J. T. Yen, "Design and in vitro evaluation of a real-time catheter localization system using time of flight measurements from seven 3.5 MHz single element ultrasound transducers towards abdominal aortic aneurysm procedures," *Ultrasonics*, vol. 51, no. 6, pp. 768–775, 2011.

[9] V. Kindratenko, "A survey of electromagnetic position tracker calibration techniques," *Virt. Real.: Res., Develop., Appl.*, vol. 5, no. 3, pp. 169–182, 2000.

[10] I. Gergel, T. R. D. Santos, R. Tetzlaff, L. Maier-Hein, H.-P. Meinzer, and I. Wegner, "Particle filtering for respiratory motion compensation during navigated bronchoscopy," *Proc. SPIE Med. Imag.*, vol. 7625, no. 1, pp. 76250W–76250W, 2010.

[11] K. Mori, D. Deguchi, K. Akiyama, T. Kitasaka, C. R. Maurer, Y. Suenaga, H. Takabatake, M. Mori, and H. Natori, "Hybrid bronchoscope tracking using a magnetic tracking sensor and image registration," in *Medical Image Computing and Computer-Assisted Intervention (MICCAI)*, ser. Lecture Notes In Computer Science. Berlin, Germany: Springer, 2005, vol. 3750, pp. 543–550.

[12] M. Feuerstein, T. Reichl, J. Vogel, J. Traub, and N. Navab, "Magneto-optical tracking of flexible laparoscopic ultrasound: Model-based online detection and correction of magnetic tracking errors," *IEEE Trans. Med. Imag.*, vol. 28, no. 6, pp. 951–967, Jun. 2009.

[13] A. J. Rogers, E. D. Light, D. von Allmen, and S. W. Smith, "Real-time 3d ultrasound guidance of autonomous surgical robot for shrapnel detection and breast biopsy," in *Proc. SPIE Med. Imag. 2009: Ultrason. Imag. Signal Process.*, 2009, pp. 72650O–72650O-6.

[14] A. Chung, P. Edwards, F. Deligianni, and G. Yang, "Freehand cocalibration of optical and electromagnetic trackers for navigated bronchoscopy," in *Proc. Int. Workshop Med. Imag. Augment. Reality*, 2004, vol. 3150, pp. 320–328.

[15] F. Conti, J. Park, and O. Khatib, "Interface design and control strategies for a robot assisted ultrasonic examination system," presented at the Int. Symp. Exp. Robot., New Delhi, India, Dec. 2010.

[16] J. Chang, B. Wen, P. Zanzonico, P. Kazanzides, R. Finn, G. Fichtinger, and C. C. Ling, "A robotic system for ^{18}F-FMISO PET—guided intratumoral pO_2 measurements," *Med. Phys.*, vol. 36, no. 11, pp. 5301–5309, 2009.

[17] F. Raab, E. Blood, T. Steiner, and H. Jones, "Magnetic position and orientation tracking system," *IEEE Trans. Aerospace Electron. Syst.*, vol. 15, no. 5, pp. 709–718, Sep. 1979.

[18] R. Y. Tsai and R. K. Lenz, "A new technique for fully autonomous and efficient 3d robotics hand/eye calibration," *IEEE Trans. Robot. Automat.*, vol. 5, no. 3, pp. 345–358, Jun. 1989.

[19] D. D. Frantz, A. D. Wiles, S. E. Leis, and S. R. Kirsch, "Accuracy assessment protocols for electromagnetic tracking systems," *Phys. Med. Biol.*, vol. 48, no. 14, pp. 2241–2251, Jul. 2003.

[20] J. B. Hummel, M. R. Bax, M. L. Figl, Y. Kang, C. Maurer Jr., W. W. Birkfellner, H. Bergmann, and R. Shahidi, "Design and application of an assessment protocol for electromagnetic tracking systems," *Med. Phys.*, vol. 32, no. 7, pp. 2371–2379, Jul. 2005.

[21] C. Nafis, V. Jensen, L. Beauregard, and P. Anderson, "Method for estimating dynamic EM tracking accuracy of surgical navigation tools," in *Proc. SPIE Medical Imag. 2006: Visualizat., Image-Guided Procedures, Display*, 2006, vol. 6141, p. 61410K.

[22] Z. Yaniv, E. Wilson, D. Lindisch, and K. Cleary, "Electromagnetic tracking in the clinical environment," *Med. Phys.*, vol. 36, no. 3, pp. 876–892, 2009.

[23] I. Gergel, J. Gaa, M. Müller, H.-P. Meinzer, and I. Wegner, "A novel fully automatic system for the evaluation of electromagnetic tracker," in *Proc. SPIE Med. Imag.*, 2012, vol. 8316, p. 831608.

[24] Aurora compact field generator data sheet Northern Digital, Waterloo, Canada.

[25] C. R. Maurer, J. M. Fitzpatrick, M. Y. Wang, R. L. Galloway, R. J. Maciunas, and G. S. Allen, "Registration of head volume images using implantable fiducial markers," *IEEE Trans. Med. Imag.*, vol. 16, no. 4, pp. 447–462, Aug. 1997.

[26] J. Hummel, M. Figl, M. Bax, R. Shahidi, H. Bergmann, and W. Birkfellner, "Evaluation of dynamic electromagnetic tracking deviation," in *Proc. SPIE Med. Imag.*, M. I. Miga and K. H. Wong, Eds., 2009, vol. 7261, pp. 72612U–72612U.

[27] L. Maier-Hein, A. M. Franz, W. Birkfellner, J. Hummel, I. Gergel, I. Wegner, and H.-P. Meinzer, "Standardized assessment of new electromagnetic field generators in an interventional radiology setting," *Med. Phys.*, vol. 39, no. 6, pp. 3424–3434, 2012.

[28] J. Hummel, M. Figl, W. Birkfellner, M. R. Bax, R. Shahidi, C. R. Maurer, Jr., and H. Bergmann, "Evaluation of a new electromagnetic tracking system using a standardized assessment protocol," *Phys. Med. Biol.*, vol. 51, no. 10, pp. 205–210, May 2006.

[29] M. A. Nixon, B. C. McCallum, W. R. Fright, and N. B. Price, "The effects of metals and interfering fields on electromagnetic trackers," *Presence: Teleoperators Virt. Environ.*, vol. 7, no. 2, pp. 204–218, 1998.

[30] R. Taylor, H. Paul, P. Kazanzides, B. Mittelstadt, W. Hanson, J. Zuhars, B. Williamson, B. Musits, E. Glassman, and W. Bargar, "Taming the bull: Safety in a precise surgical robot," in *Proc. 5th Int. Conf. Adv. Robot.*, Jun. 1991, vol. 1, pp. 865–870.

[31] W. Birkfellner, F. Watzinger, F. Wanschitz, R. Ewers, and H. Bergmann, "Calibration of tracking systems in a surgical environment," *IEEE Trans. Med. Imag.*, vol. 17, no. 5, pp. 737–742, Oct. 1998.

[32] M. Nakamoto, K. Nakada, Y. Sato, K. Konishi, M. Hashizume, and S. Tamura, "Intraoperative magnetic tracker calibration using a magneto-optic hybrid tracker for 3-D ultrasound-based navigation in laparoscopic surgery," *IEEE Trans. Med. Imag.*, vol. 27, no. 2, pp. 255–270, Feb. 2008.